Published in final edited form as:
Aquat Toxicol. 2009 August 13; 94(1): 47–55. doi:10.1016/j.aquatox.2009.05.015.

Interaction of fish aryl hydrocarbon receptor paralogs (AHR1 and AHR2) with the retinoblastoma protein

Rebeka R. Merson[a,b,*], **Sibel I. Karchner**[a], and **Mark E. Hahn**[a]

[a]Biology Department, Woods Hole Oceanographic Institution, Woods Hole, Massachusetts 02543 USA.

[b]Biology Department, Rhode Island College, 500 Mt. Pleasant Ave., Providence, Rhode, Island 02908 USA.

Abstract

The aryl hydrocarbon receptor (AHR) mediates the toxic effects of 2,3,7,8-tetrachlorodibenzo-*p*-dioxin (TCDD) and related compounds. In some mammalian cell lines, TCDD induces G1 cell cycle arrest, which depends on an interaction between the AHR and the retinoblastoma tumor suppressor (RB). Mammals possess one AHR, whereas fishes possess two or more AHR paralogs that differ in the domains important for AHR-RB interactions in mammals. To test the hypothesis that fish AHR paralogs differ in their ability to interact with RB, we cloned *RB* cDNA from Atlantic killifish, *Fundulus heteroclitus*, and studied the interactions of killifish RB protein with killifish AHR1 and AHR2. In coimmunoprecipitation experiments, *in vitro*-expressed killifish RB coprecipitated with both AHR1 and AHR2. Consistent with these results, both killifish AHR1 and AHR2 interacted with RB in mammalian two-hybrid assays. These results suggest that both fish AHR1 and AHR2 paralogs may have the potential to influence cell proliferation through interactions with RB.

Keywords

AHR; RB; tumor suppressor; marine fish; teleost; environmental toxicology

Introduction

Environmental contaminants including 2,3,7,8-tetrachlorodibenzo-*p*-dioxin (TCDD) and some polycyclic aromatic hydrocarbons (PAHs) alter gene expression and cause toxicity through the activation of the aryl hydrocarbon receptor (AHR) signaling pathway (Fujii-Kuriyama and Mimura, 2005; Schmidt and Bradfield, 1996). The AHR is a member of the basic helix-loop-helix PER-ARNT-SIM (bHLH-PAS) protein superfamily of developmental regulators and environment sensors (Gu et al., 2000). Upon activation by a ligand, the AHR enters the nucleus, dimerizes with the AHR nuclear translocator (ARNT) and binds *cis*-acting AHR-responsive elements (AHRE), also known as dioxin-responsive enhancers (DREs) and xenobiotic responsive elements (XREs), to regulate genes encoding xenobiotic metabolizing enzymes

*Corresponding author: Biology Department, Rhode Island College, 500 Mt. Pleasant, Ave., Providence, Rhode Island 02908 USA. Tel. (401) 456-8906, Fax. (401) 456-9620, rmerson@ric.edu.

(e.g., CYP1A1, CYP1A2, NQO1, ALDH3A1, UGT1A6) (Nebert et al., 2000). Additionally, numerous other genes not commonly associated with xenobiotic metabolism are regulated by AHR in response to TCDD exposure (Tijet et al., 2006).

The AHR signaling pathway has been implicated in regulation and dysregulation of the cell cycle; however, the molecular mechanisms of this regulatory role are unclear. Activation of the AHR by TCDD results in AHR-dependent G1 cell cycle arrest in cells (Weiss et al., 1996) and apoptosis in vertebrate embryos (Cantrell et al., 1998), but promotes growth and immortalization of human keratinocytes (Ray and Swanson, 2004). Mice with constitutively-active AHR develop tumors (Andersson et al., 2002) and in AHR deficient cells, proliferation rates are reduced and S-phase and M-phase transitions are delayed (Ma and Whitlock, 1996). These incongruous effects of AHR activation remain an enigma, but clearly indicate that the AHR pathway intersects multiple pathways that regulate the cell cycle (Marlowe et al., 2008; Marlowe and Puga, 2005; Puga et al., 2008).

The retinoblastoma tumor suppressor protein (RB) restricts the transition from G1 to S phase (Cobrinik et al., 1992) by sequestering E2F, a transcription factor that regulates the genes necessary for cell cycle progression from G1 phase to S phase (e.g., thymidine kinase, DNA polymerase α). Inactivation or mutation of the RB gene is observed in tumors from a diverse array of tissues and chemically-induced retinoblastoma tumors in a bony fish model (Rotchell et al., 2001). The RB protein binds to more than 20 proteins that possess an LXCXE motif, including CCND1 (Kato et al., 1993) and HDAC1 (Brehm et al., 1998). Viral oncoproteins such as papillomavirus E7 (Nevins, 1992), adenovirus E1A (Egan et al., 1988), and Simian virus 40 (SV40) large T antigen (Kim et al., 2001), inactivate RB by sequestration through a direct interaction of an LXCXE motif with RB residues Tyr709, Lys713, Tyr756, and Asn757 (Dahiya et al., 2000).

Mammalian AHR interacts with RB through the LXCXE and a region in the C-terminal transactivation domain (TAD). A high affinity site is located at the N-terminal half of the human and mouse AHR between amino acids 330 and 340, a region that contains an LXCXE motif (Elferink et al., 2001; Ge and Elferink, 1998; Puga et al., 2000). A lower affinity binding site is located between amino acids 589 and 672 in the glutamine-rich transactivation domain (Elferink et al., 2001; Ge and Elferink, 1998; Puga et al., 2000). AHR ligand binding is not necessary for RB interaction (Ge and Elferink, 1998), but nuclear translocation of AHR, which occurs following ligand binding, is a prerequisite (Puga et al., 2000). Interactions of RB and AHR enhance RB repression of E2F-dependent gene expression (Ge and Elferink, 1998; Puga et al., 2000). The proximate mechanism of cell arrest involving the AHR-RB complex is not well understood, but may involve the displacement of p300 from the promoters of genes necessary for S-phase (Marlowe et al., 2004), or the induction of genes encoding cyclin-dependent kinase inhibitors (Huang and Elferink, 2005; Kolluri et al., 1999).

Identification of specific roles of AHR in physiology can reveal the mechanisms of TCDD-induced cell cycle dysregulation. One approach to understanding the various roles of the AHR is to investigate the similarities and differences in properties of the AHR paralogs in species such as fish that have multiple AHRs. It is possible that the multiple functions of the ancestral AHR and the single mammalian AHR may be partitioned among the fish AHR paralogs (Karchner et al., 1999).

The Atlantic killifish *Fundulus heteroclitus* expresses two AHR paralogs, AHR1 and AHR2 (Karchner et al., 1999), which arose from an early vertebrate gene duplication event (Hahn et al., 2006). Piscine AHR1 is hypothesized to be orthologous to the single mammalian AHR, whereas AHR2 is paralogous to mammalian AHR and fish AHR1. The amino acid sequence in the putative high affinity RB binding domain of mammalian AHR (LXCXE) is conserved

in fish AHR1, but not in fish AHR2 (Fig. 1). The C-terminal transactivation domain of killifish AHR1 is rich in glutamine residues, as is the putative low affinity RB-binding site in the C-terminal half of mammal AHR; in contrast, the transactivation domain of the killifish AHR2 diverges from the killifish AHR1 in amino acid sequence and is not as enriched with glutamines (Karchner et al., 1999). Based on these observations, we hypothesized that killifish AHR1 plays a role in cell cycle regulation through a direct protein-protein interaction with RB, while its paralog, AHR2, has other functions that may not involve an interaction with RB. To test the hypothesis that killifish RB interacts with killifish AHR1 but not AHR2, and to expand the use of the killifish model in mechanistic studies of molecular toxicology and carcinogenesis, we cloned the retinoblastoma cDNA from killifish and assessed the ability of RB to interact with each killifish AHR *in vitro* and in mammalian cell culture-based assays.

2. Materials and Methods

2.1. RT-PCR and cDNA cloning

Fish were euthanized by cervical transection and tissues were immediately excised, frozen in liquid nitrogen or preserved in RNALater (Ambion, Austin, TX). Total RNA was isolated using Stat-60 (Tel-Test, Friendswood, TX). Messenger RNA was purified from total RNA using Mini-Oligo d(T) Cellulose Spin Column (5 Prime-3 Prime, Boulder, CO) or Oligotex mRNA Spin Columns (Qiagen, Valencia, CA) following manufacturers' instructions. Random hexamers were used to synthesize cDNA from liver mRNA and an initial fragment of RB cDNA was amplified with the GeneAmp RNA RT-PCR Kit (Applied Biosystems, Foster City, CA) using degenerate primers D5F and D4R and a subsequent nested PCR with primer pair D3F and D4R (Table 1) using cycling parameters described in Table 2. PCR products were cloned into pGEM-T Easy vector (Promega, Madison,WI) and sequenced. The resulting sequences were used to design gene-specific primers to obtain the 3'- and 5'- cDNA ends and amplify the full-length cDNA from the translation start site to the termination codon. The full-length cDNA synthesized (Omniscript RT, Qiagen) from total RNA from ovary was amplified with EcoRIkozFL-F and XhoIFL-R (Table 1), cloned, sequenced, and subcloned into *Eco*RI and *Xho*I sites of pcDNA3.1/Zeo+ (Invitrogen, Carlsbad, CA) to make the construct pcDNA-FhRB.

2.2. Tissue mRNA expression of RB assessed by real-time RT-PCR

A mixture of oligo (dT) and random hexamers was used with Omniscript RT to synthesize cDNA from 2 μg total RNA isolated from heart, spleen, kidney, brain, liver, gut, gill, and ovary of three female killifish, and the testis of three male killifish. Quantitative, real-time PCR was performed using iQ SYBR Green Supermix (Bio-Rad, Hercules, CA) with primers listed in Table 1 with cycling conditions described in Table 2, which targeted an 88 bp amplicon of killifish RB spanning junction of exons 8 and 9 predicted from human RB gene (GenBank accession no. M28419), and a 111 bp amplicon spanning exons 3 and 4 of the killifish β-actin (ACTB) (invariant internal control). A serial dilution (10^9 to 10^5 molecules/μl) of plasmids constructs containing killifish RB (pcDNAFhRB) and ACTB cDNAs were used to generate standard curves for quantification of starting material.

2.3. Coimmunoprecipitation

Full-length killifish RB was synthesized *in vitro* using the TNT® Quick Coupled Transcription/Translation System (TNT) (Promega) in the presence of 20.4 μM L-[^{35}S]Methionine (>1000 Ci/mmol, *in vivo* cell labeling grade, GE Healthcare Bio-sciences, Piscataway, NJ) and full-length killifish AHR1 (pcDNA-FhAHR1*1) and AHR2 (pcDNA-FhAHR2) were synthesized with 20 μM unlabeled methionine. *In vitro*-synthesized RB (115 μl), AHR1 (100 μl), and AHR2 (100 μl) proteins were each diluted to 200 μl in immunoprecipitation (IP) buffer (25 mM HEPES, 1.2 mM EDTA, 200 mM NaCl, 10% glycerol, 0.1% Nonidet P-40) and precleared

with 10 µl normal rabbit serum for 30 minutes at 4 °C with gentle rocking followed by adsorption with 20 µl of a 50% suspension of protein A agarose (prewashed in IP buffer) for 30 minutes at 4 °C with gentle rocking. Cleared proteins were collected by centrifugation through Handee cup spin column (Pierce, Rockford, IL). Mixtures of 75 µl AHR1 or AHR2 and 50 µl RB were diluted with 275 µl IP buffer. Half of each protein mixture was added to 10 µl specific polyclonal antibodies to killifish AHR1 and AHR2 (Merson et al., 2006) and the other half to 10 µl preimmune serum and incubated for 1 hour at 4 °C with gentle rocking. Protein-antibody mixtures were adsorbed with 30 µl IP buffer-washed protein A agarose for 1 hour at 4 °C. Protein A agarose complexes were collected by centrifugation at 1000 × g for 2 minutes. Pellets were washed 3 times with 500 µl ice-cold IP buffer, eluted from protein A with protein sample treatment buffer containing 5% 2-mercaptoethanol (Sigma, St. Louis, MO), and resolved on 8% denaturing SDS-polyacrylamide gel.

2.4. Protein-protein interaction mammalian two-hybrid experiment

Hybrid expression plasmids were constructed with the Mammalian Two Hybrid Kit (Stratagene, La Jolla, CA). Prey construct pCMVAD-FhRB was designed to express full-length RB protein fused to the NF-kB activation domain. Bait constructs pCMVBD-FhAHR1 and pCMVBD-FhAHR2 encode the GAL4 DNA-binding domain fused to killifish AHRs lacking the AHR DNA-binding domain, using killifish AHR cDNAs described previously (Karchner et al., 1999). A fragment of killifish AHR1 cDNA encoding amino acids 103-stop codon was generated by digesting pGEMFhAHR1 with *BglII* and *BstEI* and pcDNAFhAHR1 with *BstEI* and *XhoI*, ligating the *BstE1* overhangs and then inserting it into *BamHI* and *SalI* cut pCMVBD. Similarly, AHR2 cDNA encoding amino acids 84-stop codon was constructed by digesting pGEMFhAHR2 with *BamHI* and *SacI* and pcDNAFhAHR2 with *SacI* and *XhoI*, ligating the fragments and inserting them into *BamHI* and *SalI* sites of pCMVBD. pCMVAD-FhRB was generated by excising full length RB from pcDNAFhRB (described in cloning methods) and inserting into the *EcoRI* and *XhoI* sites of pCMVAD. All expression constructs were propagated and verified by sequencing.

COS-7 cells (American Type Culture Collection; Manassas, VA) were maintained in Dulbecco's Modified Eagle Medium (Sigma) and CV-1 cells were maintained in Eagle's Minimum Essential Medium (Sigma), both supplemented with 10% fetal bovine serum (Invitrogen), in a humidified incubator at 37 °C, 5% CO_2. Cells plated in complete medium on 48-well plates (3.0×10^4 cells per well) were grown for 24 hours before transfection. CV-1 cells, which lack SV40T, were used for both the interaction experiment and to establish the negative control interaction. Additionally, COS-7 cells were used to establish that interaction results are reproducible in a second cell line; previous studies showed that killifish AHRs are functional in COS-7 (Karchner et al, 2002; Hahn et al, 2004). Cells were transiently transfected (Lipofectamine 2000, Invitrogen) with 150 ng/well pFR-Luc encoding a firefly luciferase reporter gene (Stratagene) under the control of 5 GAL4 response elements, 3 ng/well pRL-TK *Renilla* luciferase transfection control plasmid, and constructs encoding the fusion proteins pCMVBD-FhAHR1 (10 ng/well in CV-1, 1 ng/well in COS-7), pCMVBD-FhAHR2 (1 ng/well in CV-1, 0.05 ng/well in COS-7), and pCMVAD-FhRB (10, 100, or 250 ng/well in CV-1 and COS-7). An additional control for non-specific interactions was included in the experiments by co-transfection of AHR or RB fusion constructs with constructs of proteins with no previously demonstrated interaction: pCMVAD-SV40 (Stratagene, amino acids 84–708 of Simian virus 40 large T-antigen) was co-transfected with pCMVBD-FhAHR1 or pCMVBD-FhAHR2 and pCMVBD-p53 (Stratagene, amino acids 72–390 of murine TP53) was co-transfected with pCMVAD-FhRB. Five hours later cells were treated with 0.5% DMSO (Sigma) or 10 nM TCDD (Ultra Scientific, N. Kingstown, RI) in triplicate wells.

Twenty-four hours after transfection (18 hours after dosing), medium was removed and the wells rinsed with 500 µl phosphate buffered saline. Cells were lysed with 100 µl Passive Lysis Buffer (Promega) with shaking at room temperature for 20 minutes. The Dual-Luciferase® Reporter Assay System (Promega) was used to measure both firefly (experimental) and *Renilla* (transfection control) luciferase activities in a TD 20/20 DLReady Luminometer (Turner BioSystems, Sunnyvale, CA).

2.5. Statistical analyses

GraphPad Prism 4.0 was used for all statistical comparisons. Experimental luciferase activity was normalized to *Renilla* luciferase activity and the ratios were analyzed with one-way ANOVA followed by Dunnett's post-test to determine significant increases in reporter activity in cells co-transfected with pCMVAD-FhRB and pCMVBD-FhAHR1 or pCMVBD-FhAHR2 compared to those transfected with AHR constructs alone. Two-way analysis of variance was used to investigate the interaction among chemical (DMSO v. TCDD) and the transfection (amount of expression construct) treatments.

3. Results and Discussion

In mammalian systems, TCDD exposure can result in either cell proliferation or arrest, and these enigmatic effects appear to depend on an intact AHR signaling pathway (Ge and Elferink, 1998; Puga et al., 2000). One proposed mechanism for AHR-dependent TCDD-induced cell cycle arrest involves a protein-protein interaction between AHR and the tumor suppressor protein RB (Ge and Elferink, 1998; Puga et al., 2000), a key regulator of the transition from G1 to S phase. Bony fishes possess two or more paralogs of the AHR, whose sequences differ in the regions that are likely to be involved in RB interaction. To investigate the pleiotropic roles of the AHR in cell cycle regulation, we identified and characterized the killifish RB. We hypothesized that the conserved residues in mammalian AHRs that allow interaction with RB would also be essential in the interaction of the AHR and RB in bony fishes. We therefore tested the ability of the killifish AHR1 and AHR2 to interact with killifish RB.

3.1. Cloning of killifish retinoblastoma tumor suppressor cDNA

To investigate the interaction of killifish AHRs with RB, we first sought to identify and characterize the *RB* homolog from killifish. A cDNA fragment encoding RB was amplified from killifish liver and ovary mRNA by RT-PCR using degenerate primers, and the full-length RB cDNA sequence was obtained by amplification of cDNA ends and PCR of the coding cDNA from the translation start site to the termination codon. The resulting cDNA of 4320 bp has an open reading frame of 2739 bp encoding a 913 amino acid protein with a predicted molecular mass of 103.5 kDa (Fig. 2; GenBank accession no. AY509123). Two cloned RACE fragments contained intron sequences in splice positions corresponding to those preceding exons 15 and 18 of the human retinoblastoma gene (Hong et al., 1989), indicating conservation of at least two mRNA splice sites among vertebrates.

The amino acid sequence of killifish RB is well conserved in comparison to RB proteins of other vertebrates, underscoring the importance of its function in cell cycle regulation. Killifish RB shares an overall amino acid identity of 48%, 67%, and 75% with RB proteins from human, trout, and medaka, respectively (Fig. 3). The large pocket sequence (amino acids 365–783) is 60, 72, and 78 % identical to that of human, trout, and medaka RB proteins, respectively. Killifish RB is well-conserved in the functionally important domains of the mammalian RB: LXCXE motif-binding residues (Dahiya et al., 2000), A and B pockets (Cobrinik et al., 1992), cyclin-recognition sequences and putative S/T phosphorylation sites (Adams, 2001), and the leucine zipper (Hong et al., 1989).

3.2. Tissue expression of retinoblastoma mRNA

The mammalian RB gene is expressed in all tissues because of its indispensable role in regulating cell proliferation. To determine the expression levels of the RB gene in killifish tissues, quantitative RT-PCR experiments were performed with three independent biological samples. RB mRNA was expressed in all killifish tissues examined. The level of RB mRNA expression varied among the tissues (Fig. 4), possibly due to differences in the proliferation status of the cells in each tissue.

3.3. Killifish RB interacts with both AHR1 and AHR2

RB interacts with the LXCXE motif and the glutamine-rich TAD of mammalian AHR in mammals (Ge and Elferink, 1998; Puga et al., 2000). Killifish AHR1 possesses both of these RB-interaction sites, but they are not conserved in AHR2 (Karchner et al., 1999) and Fig. 1). To test the ability of the killifish RB to interact with killifish AHR1 and AHR2, we conducted coimmunoprecipitation experiments using *in vitro*-synthesized full-length AHR proteins and AHR-specific antibodies. Killifish RB co-precipitated with both AHR1 and AHR2 (Fig. 5), suggesting that it is capable of interacting with both AHR paralogs.

To further assess the ability of killifish RB to interact with the AHR1 and AHR2 proteins, mammalian two-hybrid experiments were conducted in COS-7 cells and CV-1 cells transiently transfected with RB and AHR fusion constructs (Fig. 6A). If bait and target proteins interact, they reconstitute a functional complex that can induce the luciferase reporter through activation of the GAL4 response elements. As a positive control, we used pCMVAD-SV40T and pCMVBD-p53, each of which was ineffective if transfected alone (Fig. 6B, columns 14–16 and 23–24), but together interacted to activate luciferase expression (Fig. 6B, column 2). The experiments were performed in two different cell lines, COS-7 and CV-1. Both cell lines express low levels of endogenous AHR. CV-1 cells were used for confirmation and to eliminate the possibility that endogenous SV40T proteins, which are present in COS-7 cells but not in CV-1 cells, may mask a non-specific interaction of AHR-GAL4BD and SV40T-NFκB. Similar results were obtained in each cell line (CV-1 cells, Fig. 6B; COS-7 cells, Fig. 6C). Transfection of increasing amounts of RB had no effect on transcription of the reporter construct pFR-Luc (Fig. 6B and 6C, columns 3–5). Background activation of luciferase expression by killifish AHRs was minimized by transfecting only enough of the AHR construct to produce a significant induction of the luciferase reporter with TCDD treatment (Fig. 6B and 6C, columns 6 and 10). As a negative interaction control, we co-transfected AHR1 or AHR2 with a plasmid encoding SV40T, which has never been reported to interact with AHR. There was no significant increase in reporter gene activity in CV-1 cells co-transfected with AHR and SV40T as compared to each construct alone (Fig. 6B, columns 6, 10, 14–16 vs. 17–22). Similarly, co-transfection of RB with its negative interaction control, TP53, caused no increase in luciferase activity (Fig. 6B, columns 3–5 and 23–24 vs. 25 and 26).

In cells transfected with AHR1, an increase in reporter gene expression was observed when increasing amounts of RB were co-transfected (Fig. 6B and 6C, columns 7–9). In DMSO-treated cells, luciferase activity was significantly greater in cells co-transfected with AHR1 and RB than in cells transfected with AHR1 or RB constructs alone (Fig. 6B and 6C, columns 5 and 6 vs. 9). TCDD treatment enhanced this effect, causing statistically significant induction of luciferase when AHR1 was co-transfected with RB (two-way ANOVA, interaction $p < 0.05$) (Fig. 6B, column 9; Fig. 6C, columns 8 and 9).

AHR2 also interacted with RB in these two-hybrid experiments. A significant induction of the reporter gene was observed in cells co-transfected with AHR2 and 250 ng RB as compared to cells transfected with either vector alone (Fig. 6B and 6C, column 13 vs. columns 5 and 10). As seen with AHR1, this effect was enhanced by treatment with TCDD (Fig. 6B and 6C, column

13). Together, these data show that, in both cell lines, co-transfection of RB with either AHR1 or AHR2 produced a statistically significant increase in luciferase activity as compared to each construct alone, and this interaction was enhanced by TCDD.

Our findings that killifish RB interacts with killifish AHR1, the mammalian AHR ortholog, is consistent with published literature for mammalian AHRs. In contrast, the results for AHR2 were unexpected. Because neither the LXCXE motif (Fig. 1) nor the C-terminal TAD (both thought to be involved in the AHR-RB interaction) is conserved in killifish AHR2, we were surprised to find that AHR2 was able to interact with RB both *in vitro* and in two-hybrid assays performed in mammalian cells. This suggests that either there are additional AHR domains that interact with RB, or some flexibility exists in the identity of residues in the LXCXE motif, at least in heterologous systems or *in vitro*.

Nearly all AHR1 forms identified to date in non-mammalian vertebrates contain a conserved LXCXE motif and all AHR2s are divergent in two or more residues of this motif (Fig. 1). The only exception is found in the zebrafish Ahr1a, which has MXCXE. Interestingly, unlike other AHR1 orthologs, the zebrafish Ahr1a does not bind typical AHR ligands nor does it transactivate reporter genes driven by mouse *Cyp1a* promoter (Andreasen et al., 2002;Karchner et al., 2005). AHR-RB interactions in yeast two-hybrid assays were disrupted when point mutations were made in the LXCXE motif of the mammalian AHR (Elferink et al., 2001). The chemical nature of amino acid substitutions in the killifish AHR2 (LXCXE→MXCXD) may not be sufficiently different to abolish the interaction of AHR with RB. The affinity of LXCXE motif-containing proteins for RB is partly determined by the amino acid residues flanking the LXCXE motif (Singh et al., 2005). The affinity for RB was assessed with peptides containing the LXCXE motif and flanking residues of viral oncoproteins and other LXCXE-containing proteins. In that study, RB binding depended on an extended motif XLXCXEXXX, where high affinity was conferred by X being amino acids with any side group except positively charged groups, and X being a residue with a hydrophobic side group. The killifish AHR1 and AHR2 are identical in the residues flanking the LXCXE motif, which possess the side group characteristics for high affinity binding to RB (X = His; Fig. 1). Interestingly, the histidine residue at X (corresponding to amino acid 332 of killifish AHR1) is conserved in all vertebrate and invertebrate AHRs. Experiments involving point mutations in AHR and RB and chimeric constructs will provide additional information regarding determinants of protein-protein interaction among AHR paralogs and RB.

The results of our mammalian two-hybrid experiments suggest that the presence of the AHR ligand, TCDD, enhances the ability of the killifish AHRs and RB to interact. This is consistent with previously published findings; the AHR agonist β-naphthoflavone enhanced reporter activity in yeast two-hybrid assays (Ge and Elferink, 1998; Puga et al., 2000), and AHR coprecipitated with RB in MCF-7 cells treated with TCDD, but not in control cells (Puga et al., 2000). These results suggest that ligand activation and translocation to the nucleus, where RB is located, is required for the proteins to interact in cells, and/or AHR ligand binding causes structural change to a conformation that can bind to RB; however, ligand binding is not necessary for the AHR to interact with RB *in vitro* (Puga et al., 2000).

Subfunctionalization is the evolutionary process of partitioning the multiple functions of an ancestral gene among paralogs—functional copies of genes retained following gene or genome duplication events (Force et al., 1999; Postlethwait et al., 2004). Partitioning may be manifested through complementary tissue expression or by the division of functional roles among the paralogous genes such that collectively the duplicates function as the ancestral gene (de Souza et al., 2005). AHR1 and AHR2 appear to have distinct but overlapping tissue-specific patterns of mRNA (Karchner et al., 1999) and protein expression (Merson et al., 2006), which suggests a degree of expression partitioning; whether there is also functional partitioning is not yet

known. That both AHR1 and AHR2 interact with RB suggests that they may be able to participate in cell cycle regulation; however, they may differ in the specific roles they play to facilitate the complex interactions of RB in controlling cell proliferation.

Acknowledgments

We thank Dr. Alvaro Puga for insightful discussions about AHR-RB interactions. This research was funded by National Institutes of Health, National Institute of environmental Health Sciences(NIEHS) National Research Service Award Postdoctoral Fellowship F32 ES005935 (RRM) and Transitions to Independent Positions (TIP) K22 ES014736 (RRM), and RI-INBRE Grant # P20RR016457 from the National Center for Research Resources for faculty development (RRM), NIEHS Superfund Basic Research Program at Boston University (P42ES007381 MEH), and the Oliver S. and Jennie R. Donaldson Charitable Trust (MEH and RRM). The contents are solely the responsibility of the authors and do not necessarily represent the official views of NIH.

References

Adams PD. Regulation of the retinoblastoma tumor suppressor protein by cyclin/cdks. Biochim Biophys Acta 2001;1471(3):M123–M133. [PubMed: 11250068]

Andersson P, McGuire J, Rubio C, Gradin K, Whitelaw ML, Pettersson S, Hanberg A, Poellinger L. A constitutively active dioxin/aryl hydrocarbon receptor induces stomach tumors. Proc Natl Acad Sci U S A 2002;99(15):9990–9995. [PubMed: 12107286]

Andreasen EA, Hahn ME, Heideman W, Peterson RE, Tanguay RL. The zebrafish (Danio rerio) aryl hydrocarbon receptor type 1 is a novel vertebrate receptor. Mol Pharmacol 2002;62(2):234–249. [PubMed: 12130674]

Brehm A, Miska EA, McCance DJ, Reid JL, Bannister AJ, Kouzarides T. Retinoblastoma protein recruits histone deacetylase to repress transcription. Nature 1998;391(6667):597–601. [PubMed: 9468139]

Cantrell SM, Joy-Schlezinger J, Stegeman JJ, Tillitt DE, Hannink M. Correlation of 2,3,7,8-tetrachlorodibenzo-p-dioxin-induced apoptotic cell death in the embryonic vasculature with embryotoxicity. Toxicol Appl Pharmacol 1998;148(1):24–34. [PubMed: 9465260]

Cobrinik D, Dowdy SF, Hinds PW, Mittnacht S, Weinberg RA. The retinoblastoma protein and the regulation of cell cycling. Trends Biochem Sci 1992;17(8):312–315. [PubMed: 1412705]

Dahiya A, Gavin MR, Luo RX, Dean DC. Role of the LXCXE binding site in Rb function. Mol Cell Biol 2000;20(18):6799–6805. [PubMed: 10958676]

de Souza FS, Bumaschny VF, Low MJ, Rubinstein M. Subfunctionalization of expression and peptide domains following the ancient duplication of the proopiomelanocortin gene in teleost fishes. Mol Biol Evol 2005;22(12):2417–2427. [PubMed: 16093565]

Egan C, Jelsma TN, Howe JA, Bayley ST, Ferguson B, Branton PE. Mapping of cellular protein-binding sites on the products of early-region 1A of human adenovirus type 5. Mol Cell Biol 1988;8(9):3955–3959. [PubMed: 2975755]

Elferink CJ, Ge NL, Levine A. Maximal aryl hydrocarbon receptor activity depends on an interaction with the retinoblastoma protein. Mol Pharmacol 2001;59(4):664–673. [PubMed: 11259609]

Force A, Lynch M, Pickett FB, Amores A, Yan YL, Postlethwait J. Preservation of duplicate genes by complementary, degenerative mutations. Genetics 1999;151(4):1531–1545. [PubMed: 10101175]

Fujii-Kuriyama Y, Mimura J. Molecular mechanisms of AhR functions in the regulation of cytochrome P450 genes. Biochem Biophys Res Commun 2005;338(1):311–317. [PubMed: 16153594]

Ge NL, Elferink CJ. A direct interaction between the aryl hydrocarbon receptor and retinoblastoma protein. Linking dioxin signaling to the cell cycle. J Biol Chem 1998;273(35):22708–22713. [PubMed: 9712901]

Gu YZ, Hogenesch JB, Bradfield CA. The PAS superfamily: sensors of environmental and developmental signals. Annu Rev Pharmacol Toxicol 2000;40:519–561. [PubMed: 10836146]

Hahn ME, Karchner SI, Franks DG, Merson RR. Aryl hydrocarbon receptor polymorphisms and dioxin resistance in Atlantic killifish (Fundulus heteroclitus). Pharmacogenetics 2004;14(2):131–143. [PubMed: 15077014]

Hahn ME, Karchner SI, Evans BR, Franks DG, Merson RR, Lapseritis JM. Unexpected diversity of aryl hydrocarbon receptors in non-mammalian vertebrates: insights from comparative genomics. J Exp Zoolog A Comp Exp Biol 2006;305(9):693–706.

Hong FD, Huang HJ, To H, Young LJ, Oro A, Bookstein R, Lee EY, Lee WH. Structure of the human retinoblastoma gene. Proc Natl Acad Sci U S A 1989;86(14):5502–5506. [PubMed: 2748600]

Huang G, Elferink CJ. Multiple mechanisms are involved in Ah receptor-mediated cell cycle arrest. Mol Pharmacol 2005;67(1):88–96. [PubMed: 15492120]

Karchner SI, Franks DG, Powell WH, Hahn ME. Regulatory interactions among three members of the vertebrate aryl hydrocarbon receptor family: AHR repressor, AHR1, and AHR2. J. Biol. Chem 2002;277(9):6949–6959. [PubMed: 11742002]

Karchner SI, Franks DG, Hahn ME. AHR1B, a new functional aryl hydrocarbon receptor in zebrafish: tandem arrangement of ahr1b and ahr2 genes. Biochem J 2005;392(Pt 1):153–161. [PubMed: 16042621]

Karchner SI, Powell WH, Hahn ME. Identification and functional characterization of two highly divergent aryl hydrocarbon receptors (AHR1 and AHR2) in the teleost Fundulus heteroclitus. Evidence for a novel subfamily of ligand-binding basic helix loop helix-Per-ARNT-Sim (bHLH-PAS) factors. J Biol Chem 1999;274(47):33814–33824. [PubMed: 10559277]

Kato J, Matsushime H, Hiebert SW, Ewen ME, Sherr CJ. Direct binding of cyclin D to the retinoblastoma gene product (pRb) and pRb phosphorylation by the cyclin D-dependent kinase CDK4. Genes Dev 1993;7(3):331–342. [PubMed: 8449399]

Kim HY, Ahn BY, Cho Y. Structural basis for the inactivation of retinoblastoma tumor suppressor by SV40 large T antigen. Embo J 2001;20(1–2):295–304. [PubMed: 11226179]

Kolluri SK, Weiss C, Koff A, Gottlicher M. p27(Kip1) induction and inhibition of proliferation by the intracellular Ah receptor in developing thymus and hepatoma cells. Genes Dev 1999;13(13):1742–1753. [PubMed: 10398686]

Ma Q, Whitlock JPJ. The aromatic hydrocarbon receptor modulates the Hepa-1c1c7 cell cycle and differentiated state independently of dioxin. Mol Cell Biol 1996;16:2144–2150. [PubMed: 8628281]

Marlowe JL, Fan Y, Chang X, Peng L, Knudsen ES, Xia Y, Puga A. The aryl hydrocarbon receptor binds to E2F1 and inhibits E2F1-induced apoptosis. Mol Biol Cell 2008;19(8):3263–3271. [PubMed: 18524851]

Marlowe JL, Knudsen ES, Schwemberger S, Puga A. The aryl hydrocarbon receptor displaces p300 from E2F-dependent promoters and represses S phase-specific gene expression. J Biol Chem 2004;279 (28):29013–29022. [PubMed: 15123621]

Marlowe JL, Puga A. Aryl hydrocarbon receptor, cell cycle regulation, toxicity, and tumorigenesis. J Cell Biochem 2005;96(6):1174–1184. [PubMed: 16211578]

Merson RR, Franks DG, Karchner SI, Hahn ME. Development and characterization of polyclonal antibodies against the aryl hydrocarbon receptor protein family (AHR1, AHR2, and AHR repressor) of Atlantic killifish Fundulus heteroclitus. Comp Biochem Physiol C Toxicol Pharmacol 2006;142 (1–2):85–94. [PubMed: 16364694]

Nebert DW, Roe AL, Dieter MZ, Solis WA, Yang Y, Dalton TP. Role of the aromatic hydrocarbon receptor and [Ah] gene battery in the oxidative stress response, cell cycle control, and apoptosis. Biochem Pharmacol 2000;59(1):65–85. [PubMed: 10605936]

Nevins JR. E2F: a link between the Rb tumor suppressor protein and viral oncoproteins. Science 1992;258 (5081):424–429. [PubMed: 1411535]

Postlethwait J, Amores A, Cresko W, Singer A, Yan YL. Subfunction partitioning, the teleost radiation and the annotation of the human genome. Trends Genet 2004;20(10):481–490. [PubMed: 15363902]

Puga A, Barnes SJ, Dalton TP, Chang C, Knudsen ES, Maier MA. Aromatic hydrocarbon receptor interaction with the retinoblastoma protein potentiates repression of E2F-dependent transcription and cell cycle arrest. J Biol Chem 2000;275(4):2943–2950. [PubMed: 10644764]

Puga A, Ma C, Marlowe JL. The aryl hydrocarbon receptor cross-talks with multiple signal transduction pathways. Biochem Pharmacol. 2008

Ray SS, Swanson HI. Dioxin-induced immortalization of normal human keratinocytes and silencing of p53 and p16INK4a. J Biol Chem 2004;279(26):27187–27193. [PubMed: 15111621]

Rotchell JM, Ulnal E, Van Beneden RJ, Ostrander GK. Retinoblastoma gene mutations in chemically induced liver tumor samples of Japanese medaka (Oryzias latipes). Mar Biotechnol (NY) 2001;3:S44–S49. [PubMed: 14961299]

Schmidt JV, Bradfield CA. Ah receptor signaling pathways. Annu Rev Cell Dev Biol 1996;12:55–89. [PubMed: 8970722]

Singh M, Krajewski M, Mikolajka A, Holak TA. Molecular determinants for the complex formation between the retinoblastoma protein and LXCXE sequences. J Biol Chem 2005;280(45):37868–37876. [PubMed: 16118215]

Tijet N, Boutros PC, Moffat ID, Okey AB, Tuomisto J, Pohjanvirta R. Aryl hydrocarbon receptor regulates distinct dioxin-dependent and dioxin-independent gene batteries. Mol Pharmacol 2006;69 (1):140–153. [PubMed: 16214954]

Weiss C, Kolluri SK, Kiefer F, Göttlicher M. Complementation of Ah receptor deficiency in hepatoma cells: Negative feedback regulation and cell cycle control by the Ah receptor. Exp Cell Res 1996;226:154–163. [PubMed: 8660951]

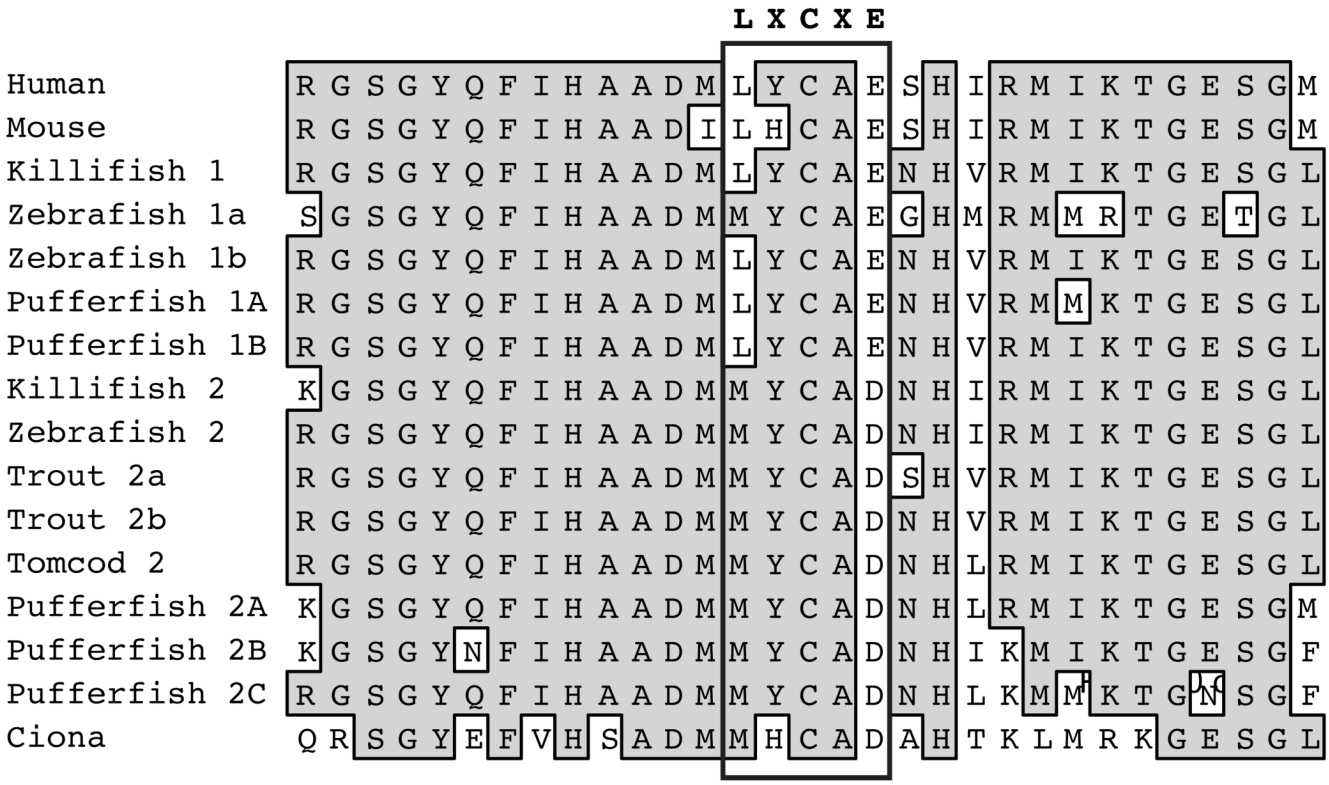

Figure 1. Sequence alignment of LXCXE motif of AHR homologs

Accession no. human L19872, mouse M94623, killifish 1 AF024591, zebrafish 1a AF258854, zebrafish 1b DQ016494, pufferfish 1A DQ088137, pufferfish 1B DQ088138, killifish 2 U29679, zebrafish 2 AF063446, trout 2α AF065137, trout 2β AF065138, tomcod AF050489, pufferfish 2A DQ088139, pufferfish 2B DQ088140, pufferfish 2C DQ088141, *Ciona* AHR NP001071651. Amino acids are numbered and shaded positions indicate >60% identity.

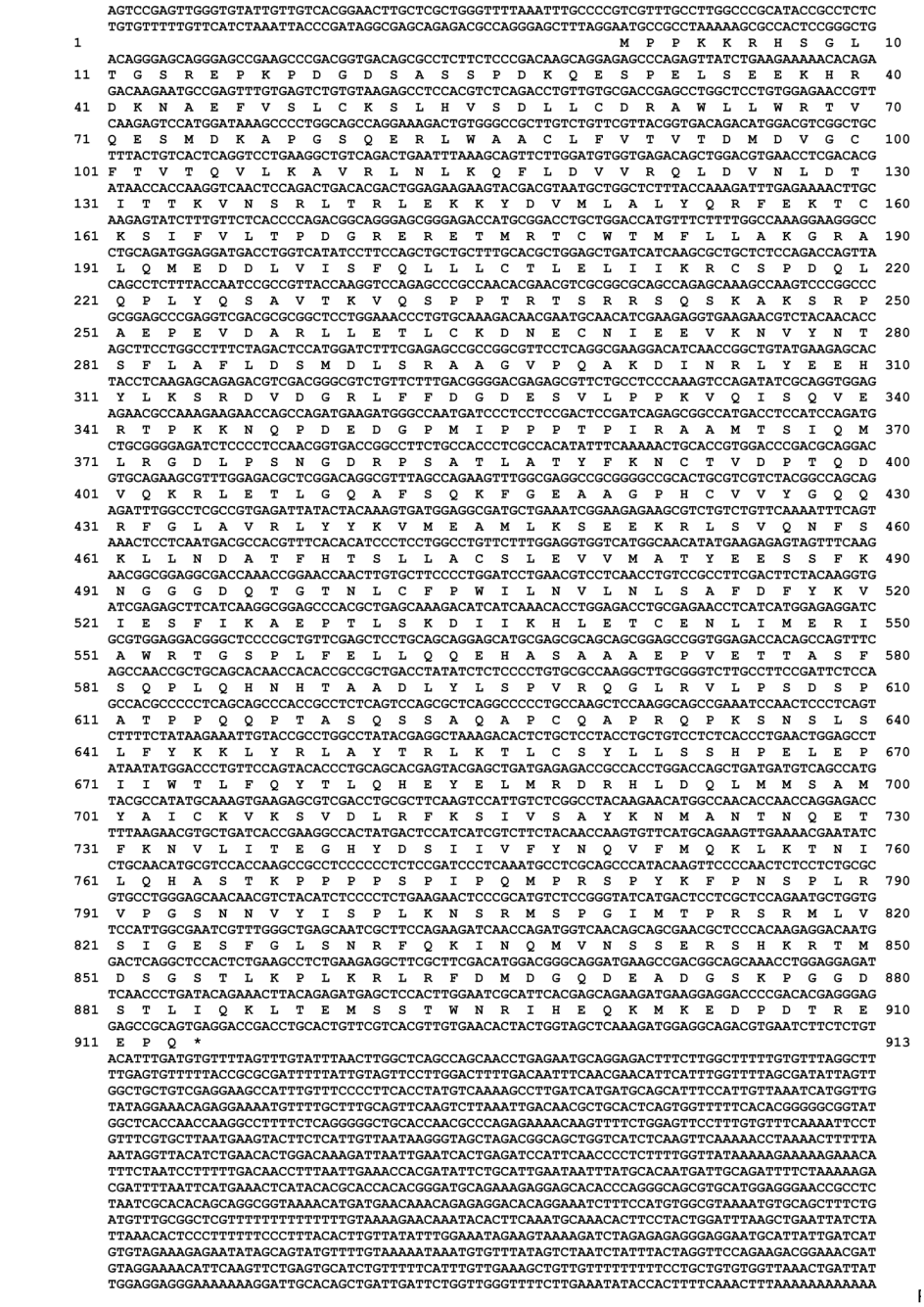

Figure 2. Nucleotide and deduced amino acid sequence of killifish RB cDNA

Amino acids are numbered and asterisk (*) indicates the stop codon. This sequence is deposited in GenBank under accession # AY509123.

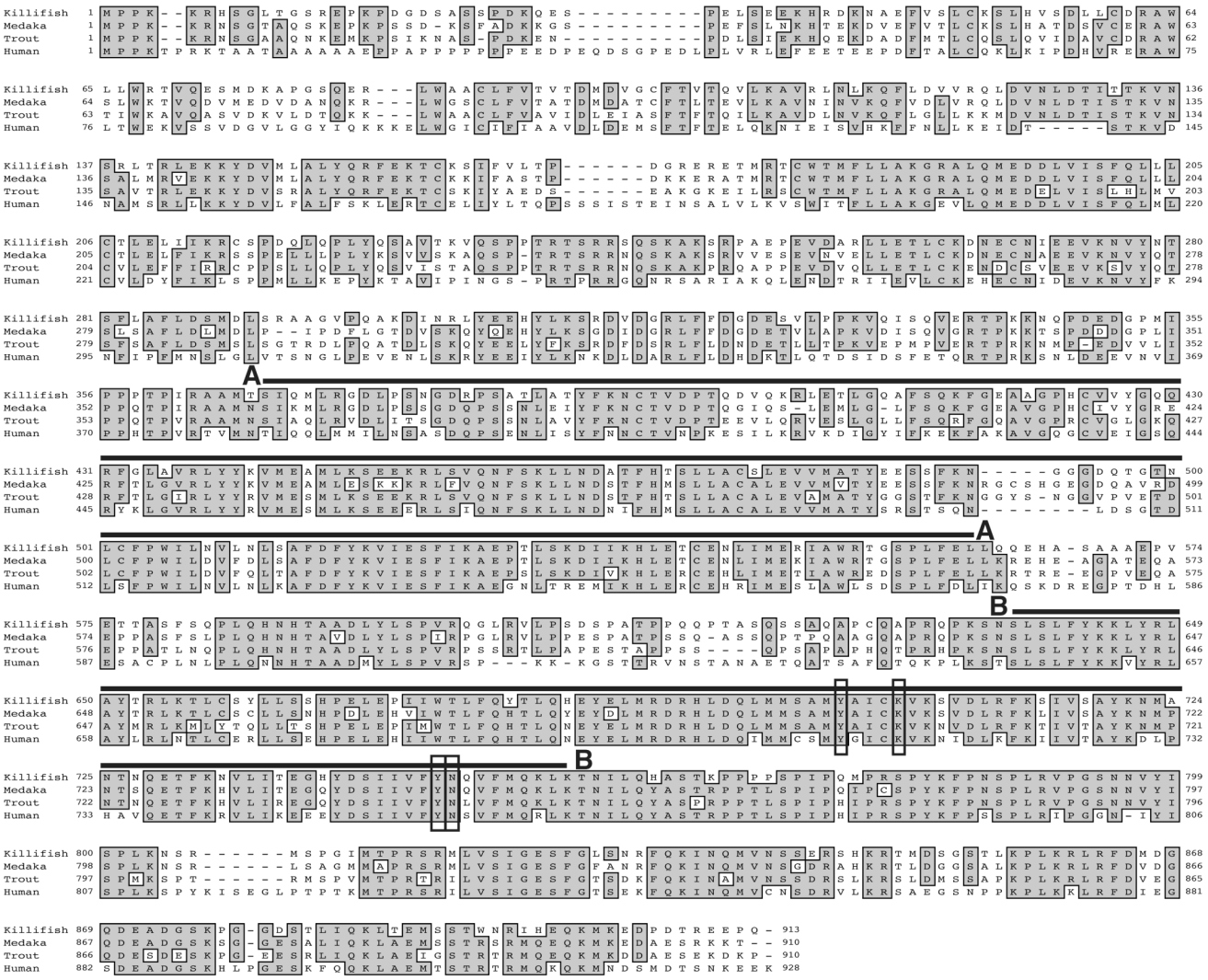

Figure 3. Alignment of RB amino acid sequences

Alignment of the retinoblastoma proteins (RB) of killifish, human (accession no. P06400), trout (accession no. AF102861), and medaka (accession no. AY008289). Shading indicates amino acid identity ≥75%. The A and B regions of the RB pocket domain, listed in the Sanger Pfam database (http://pfam.sanger.ac.uk/) as pf01858 and pf01857, respectively, of human RB are marked. Amino acid residues of RB that interact with the LXCXE motif are enclosed in boxes.

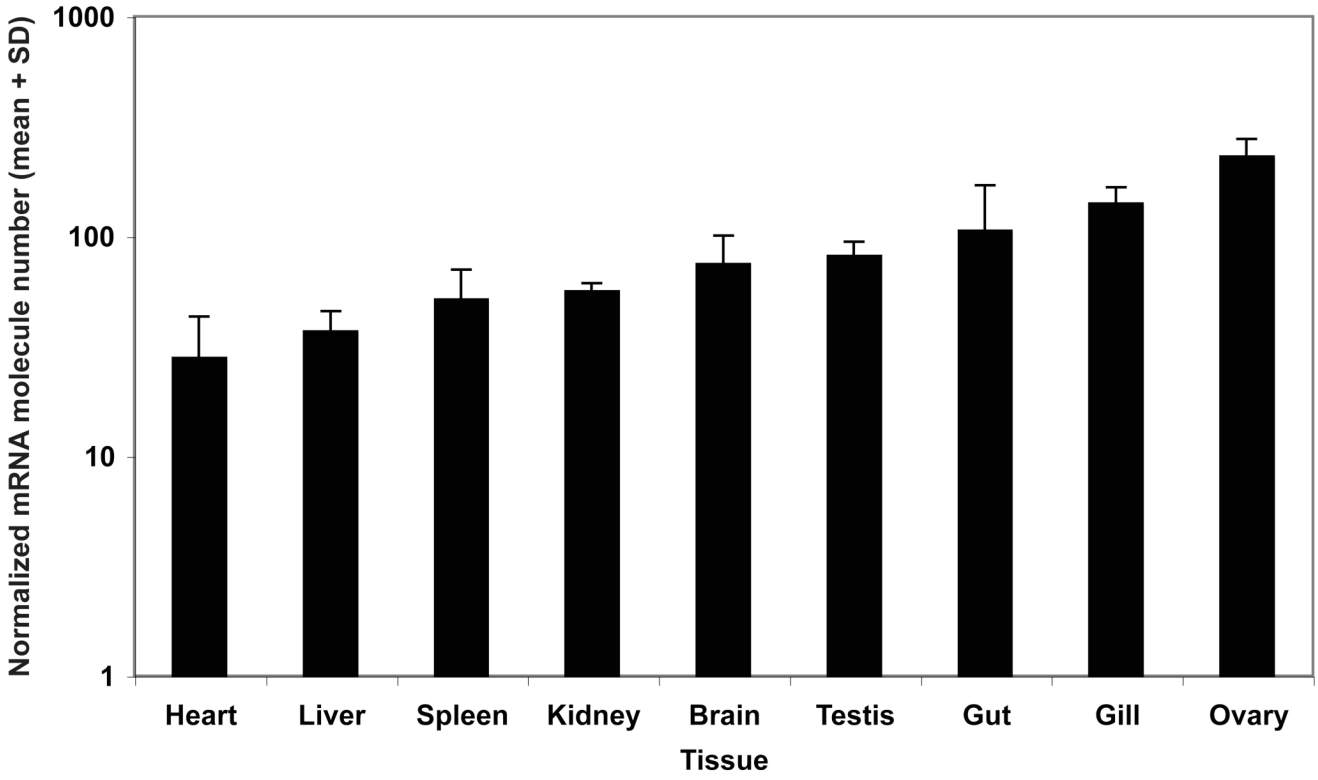

Figure 4. Expression of RB in killifish tissues

Quantitative PCR was used to determine expression of RB mRNA from ovary, heart, spleen, liver, kidney, brain, testes, gut, and gill tissues. Shown are mean ± 1 SD of starting molecule number for RB normalized to starting molecule number of ACTB. Data are from a representative qPCR experiment of tissue cDNAs from three female fish and testis cDNA from three male killifish.

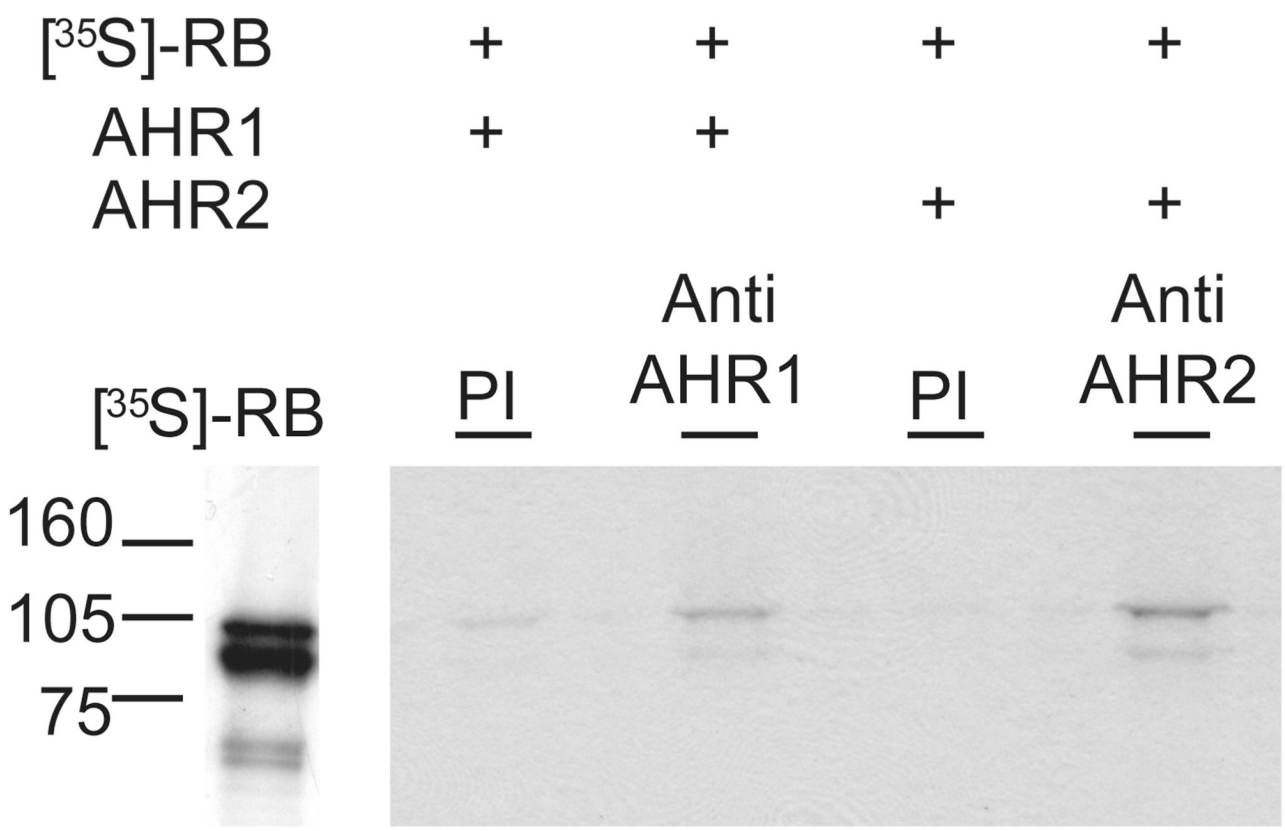

Figure 5. Coimmunoprecipitation of killifish AHRs

Co-immunoprecipitation of *in vitro* synthesized [^{35}S]-RB and AHR1 or AHR2 proteins with preimmune (normal rabbit serum) or specific polyclonal antisera. First lane shown is 5 μl of [^{35}S]-RB. Protein incubations of [^{35}S]-RB and AHR proteins are indicated with a plus (+) over the corresponding precipitate lane. Negative precipitation controls in this experiment are with serum from preimmune rabbits (essentially normal rabbit serum). Serum from rabbits generating AHR-specific polyclonal antibodies was used for specific precipitation of AHR protein complexes.

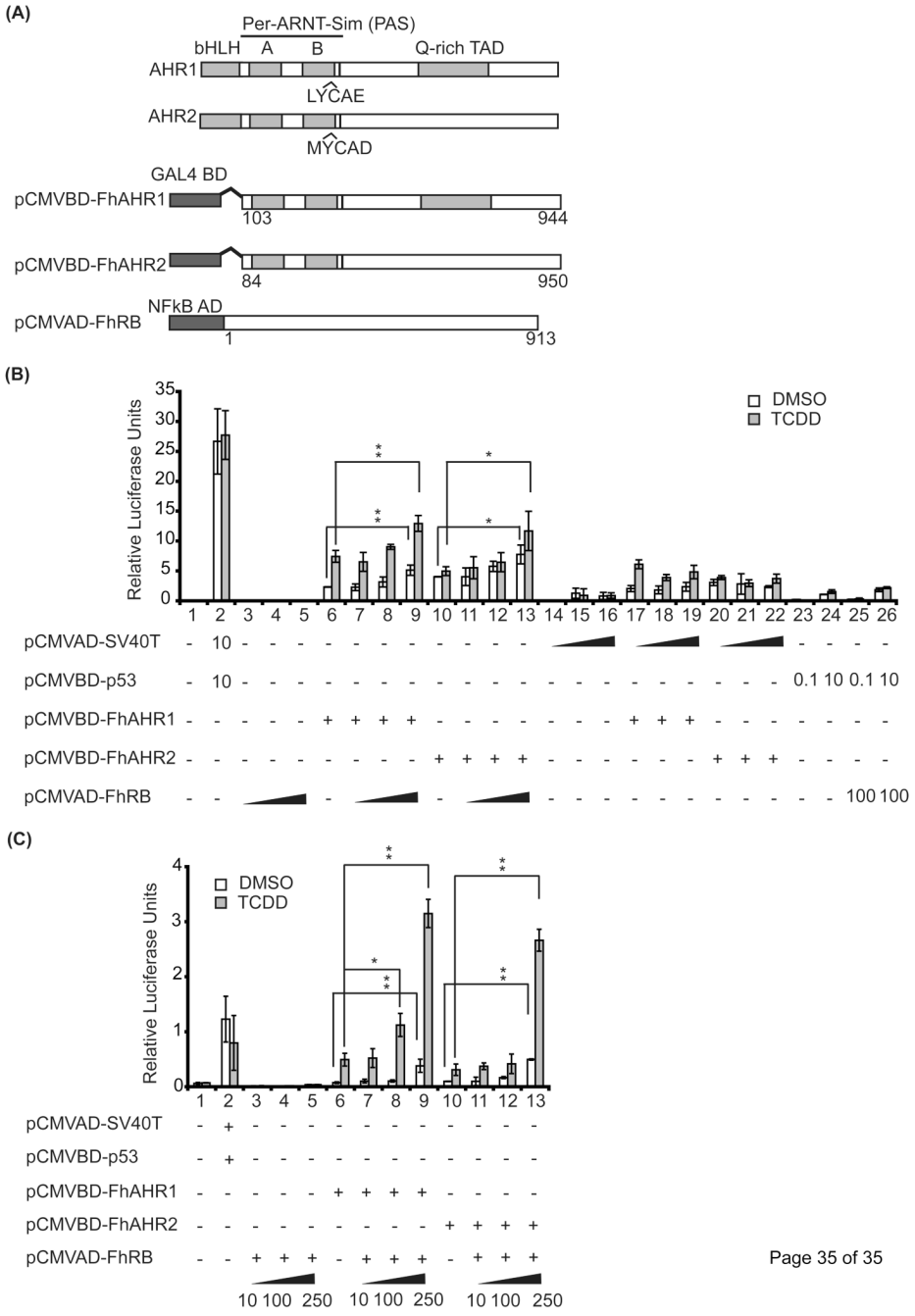

Figure 6. Protein interaction in mammalian two-hybrid assay

(A) Expression constructs used in mammalian two-hybrid assays. (B) CV-1 cells were transiently transfected with reporter and control constructs (pFR-Luc, pRL-TK), and experimental expression constructs bait pCMVBD-FhAHR1 (10 ng), pCMVBD-FhAHR2 (1.0 ng), prey pCMVAD-FhRB, or other interaction controls pCMV-p53, and pCMVAD-SV40T, and treated with DMSO or TCDD. Lines connecting treatments indicate the comparisons made in the one-way ANOVA Dunnett's post-test and p-value is indicated above the comparisons (*$p<0.05$, **$p<0.01$). (C) COS-7 cells were transiently transfected as described above, except the amount of construct DNA, pCMVBD-FhAHR1 (1.0 ng) and pCMVBD-FhAHR2 (0.05 ng). Shown is a representative of 4 independent experiments with similar results. Data

presented as mean relative luciferase units (RLU) (ratios of firefly to *Renilla* luciferase activity) ± 1 SD of triplicate wells, the amount of transfected plasmid (ng). Lines connecting treatments indicate the comparisons made in the one-way ANOVA Dunnett's post-test and p-value is indicated above the comparisons (*$p<0.05$, **$p<0.01$).

Table 1

Oligonucleotide primers used for amplification of initial RB cDNA (I), rapid amplification of cDNA ends (RACE), full-length amplification (FL), subcloning for two-hybrid construct preparation (2H), and quantitative PCR (QP).

Primer name	Nucleotide sequence (5’-3’)
D3F (I)	GACMGICACCTSGAYCARHTIATGATG
D5F (I)	TTCGACTTCTACAARGTIATHGAR
D4R (I)	GTDSAISYIATCTCIGCIARYTTYTG
1R (5’-RACE)	CAGGTAACAGAGCCGGATGTTCT
2R (5’-RACE)	GTCGGTACATGCGGTATACGTTTC
3R (5’-RACE)	GGTCGCCTCCGCCGTTCTTGAAAC
4R (5’-RACE)	CCTCCAAAGAACAGGCCAGGAGGG
7R (5’-RACE)	GTCTTTGCACAGGGTTTCCAGGAGC
8R (5’-RACE)	AAAGAGGCTGTAACTGGTCTGGAGAC
1F (3’-RACE)	GCCTCTGAAGAGGCTTCGCTTGC
2F (3’-RACE)	GCAAACCTGGAGGAGATTCAACCC
EcoRIkozFL-F (FL)	ACGGAATTCGCCACCATGCCGCCTAAAAAGCGCCA
XhoIFL-R (FL)	GTACTCGAGAGGTCGGTCCTCACTGCGGC
KpnIATG-F (2H)	GGGGTACCATGCCGCCTAAAAAGCGCC
ex8-9-F (QP)	CAACGAATGCAACATCGAAGA
ex9-R (QP)	CGGCGGCTCTCGAAAGATCC
ACTB-F (QP)	TGGAGAAGAGCTACGAGCTCC
ACTB-R (QP)	CCGCAGGACTCCATTCCGAG

Table 2

PCR cycling parameters used to amplify full-length RB cDNA, and quantitative PCR. Times listed are in minutes.

Experiment	Primers	Initial Denaturation	Denaturation Annealing	Final Extension	Cycles	Melt curve
Initial product amplification	D3F D4R	95 °C 1:45	95 °C 0:15 58 °C 0:30 72 °C 1:30	72 °C 7:00	35	N/A
Full-length amplification	EcoRIkozFL-F XholFL-R	94 °C 1:00	94 °C 1:00 66 °C 3:00	66 °C 10:00	35	N/A
Quantitative PCR	ex8-9-F ex9-R ACTB-F ACTB-R	95 °C 5:00	94 °C 0:10 68 °C 0:30	N/A	40	40 °C – 90 °C 0:30 0.5 °C increments